Translational Oncology
www.transonc.com

Volume 7 Number 6 December 2014 pp. 812–823 812

Increased Anticancer Efficacy of Intravesical Mitomycin C Therapy when Combined with a PCNA Targeting Peptide[1]

Odrun A. Gederaas*,[2], Caroline D. Søgaard*,[2], Trond Viset[†], Siri Bachke*, Per Bruheim[‡], Carl-Jørgen Arum*,[§] and Marit Otterlei*,[¶]

*Department of Cancer Research and Molecular Medicine, Norwegian University of Science and Technology, Trondheim, Norway; [†]Department of Pathology and Medical Genetics, St Olavs Hospital, Trondheim University Hospital, Trondheim, Norway; [‡]Department of Biotechnology, Norwegian University of Science and Technology, Trondheim Norway; [§]Department of Urology and Surgery, St Olavs Hospital, Trondheim University Hospital, Trondheim, Norway; [¶]APIM Therapeutics A/S, Trondheim, Norway

Abstract

Non–muscle-invasive bladder cancers (NMIBCs) are tumors confined to the mucosa or the mucosa/submucosa. An important challenge in treatment of NMIBC is both high recurrence and high progression rates. Consequently, more efficacious intravesical treatment regimes are in demand. Inhibition of the cell's DNA repair systems is a new promising strategy to improve cancer therapy, and proliferating cell nuclear antigen (PCNA) is a new promising target. PCNA is an essential scaffold protein in multiple cellular processes including DNA replication and repair. More than 200 proteins, many involved in stress responses, interact with PCNA through the AlkB homologue 2 PCNA-interacting motif (APIM), including several proteins directly or indirectly involved in repair of DNA interstrand crosslinks (ICLs). In this study, we targeted PCNA with a novel peptide drug containing the APIM sequence, ATX-101, to inhibit repair of the DNA damage introduced by the chemotherapeutics. A bladder cancer cell panel and two different orthotopic models of bladder cancer in rats, the AY-27 implantation model and the dietary BBN induction model, were applied. ATX-101 increased the anticancer efficacy of the ICL-inducing drug mitomycin C (MMC), as well as bleomycin and gemcitabine in all bladder cancer cell lines tested. Furthermore, we found that ATX-101 given intravesically in combination with MMC penetrated the bladder wall and further reduced the tumor growth in both the slow growing endogenously induced and the rapidly growing transplanted tumors. These results suggest that ATX-101 has the potential to improve the efficacy of current MMC treatment in NMIBC.

Translational Oncology (2014) 7, 812–823

Address all correspondence to: Marit Otterlei, PhD, Professor, Department of Cancer Research and Molecular Medicine, Faculty of Medicine, Norwegian University of Science and Technology, NO-7489 Trondheim, Norway.
E-mail: marit.otterlei@ntnu.no

[1] This work was supported by the Norwegian Cancer Society, the Liaison Committee between the Central Norway Regional Health Authority and the Norwegian University of Science and Technology (NTNU), the Cancer Fund at St Olavs Hospital (Trondheim, Norway), APIM Therapeutics A/S, and the Research Council of Norway. The funders had no role in the study design, data collection and analysis, decision to publish, or preparation of the manuscript. Conflict of interest: The authors have the following interests. APIM Therapeutics, a spin-off company of the NTNU, has co-funded this study. M.O. is an inventor, minority shareholder, and chief scientific officer (CSO) in the company (Patent Application No. PCT/GB2009/000489 "New PCNA interacting motif", filed on February 20, 2009). There are no further patents, products, development, or marked products to declare.
[2] Equal contribution, alphabetical order.
Received 16 September 2014; Revised 13 October 2014; Accepted 13 October 2014

1936-5233/14
http://dx.doi.org/10.1016/j.tranon.2014.10.005

Introduction

Non–muscle-invasive bladder cancer (NMIBC) accounts for 60% to 80% of newly diagnosed bladder cancer. NMIBC with current treatment still has a high probability for relapse, ranging from 31% to 78% after 5 years. A more serious challenge in these patients is progression rates up to 45% for high-risk disease, i.e., submucosal invasion and/or carcinoma *in situ*. Consequently, new intravesical treatment regimes are in demand [1,2].

Mitomycin C (MMC) alkylates and cross-links DNA and is among the most commonly used chemotherapeutic agent in NMIBC. The DNA interstrand crosslinks (ICLs) introduced by MMC are highly cytotoxic lesions. The severity of ICLs is due to involvement of both DNA strands and thus subsequent arrest of both replication and transcription. To repair ICLs, complex mechanisms involving translesion synthesis (TLS), homologous recombination, mismatch repair, nucleotide excision repair, several endonucleases, and Fanconi anemia proteins are required [3,4].

Proliferating cell nuclear antigen (PCNA) is an essential organizer "hub" protein in DNA replication and repair [5]. PCNA has also recently been linked to various cytosolic functions such as regulation of apoptosis, metabolism, and antitumor immunity [6–8]. More than 400 proteins may interact with PCNA using two binding motifs, PCNA-interacting peptide (PIP)-box [9] and AlkB homologue 2 PCNA-interacting motif (APIM) [10]. We and others have demonstrated that functional interaction with PCNA is mediated through APIM in several DNA repair proteins important for repair of ICLs [10–14]. Hence, several lines of evidence suggest that PCNA interactions through the APIM sequence are vital during cellular stress. Therefore, blocking these interactions by targeting PCNA with APIM-containing peptides may impair the cell's ability to survive genotoxic stress introduced by chemotherapeutics and radiation therapy. A novel cell penetrating APIM-containing peptide, ATX-101, targets PCNA and reduces the binding of APIM-containing proteins to PCNA [15], thus inducing apoptosis and enhancing the efficacy of chemotherapeutic drugs in various cancer cell lines, in primary cancer cells *ex vivo*, and in xenograft models [15]. In this study, we examined if targeting PCNA with ATX-101 in bladder cancer cell lines and animal models increased the efficacy of chemotherapeutics, and if ATX-101 could penetrate the bladder wall and thus have the potential to increase the efficacy of intravesical MMC treatment in NMIBC.

Materials and Methods

Peptide

ATX-101 peptide [15] was purchased from Innovagen, (Lund, Sweden)

Chemotherapeutics

MMC (Medac, Chicago, IL, USA), bleomycin (Baxter Medical, CA, USA), and gemcitabine (Santa Cruz Biotechnology Inc, Los Angeles, CA, USA) were used in cell survival studies and in animal models as described below and in Figures 1, 2, and 4.

Cell Lines

TCCSUP, HT-1197, Um-Uc-3, HT-1376, RT4, T-24, and 5367, all urothelial carcinomas from the bladder cancer cell panel ATCC No. TCP-1020, were grown as recommended. AY-27, a syngeneic rat bladder cancer cell line, was kindly provided by Professor S. Selman, Department of Urology, Medical College of Ohio, Toledo, OH, USA. Growth conditions were as previously described [16].

Cell Survival Assay

Cells were seeded into 96-well plates, and different doses of ATX-101 and chemotherapeutic drugs were added. Cells were exposed continuously and harvested everyday for the next 4 days using the 3-(4.5-dimethylthiazol-2-yl)-2.5 diphenyltetrazolium bromide assay as previously described [15].

Orthotopic Rat Bladder Cancer Models

The AY-27 model is previously described [17,18] The BBN model is based on *N*-butyl-*N*-(4-hydroxybutyl)-nitrosamine–induced bladder cancers as described in [19,20]. Briefly, endogenous tumors were induced by continuous exposure of BBN (0.05%; Sigma, St. Louis, MO, USA) in the drinking water for 12 weeks. The animals were thereafter given normal tap water *ad libitum* and monitored daily for general health status and treated 33 days after ended BBN exposure.

Animals and Ethics

Female Fischer CDF344 rats (Harlan Laboratories, Blackthorn, United Kingdom) were used for all experiments at the Unit of Comparative Medicine, Norwegian University of Science and Technology (NTNU). The animal experiments were approved by the Norwegian National Animal Research Authority [Forsøksdyrutvalget (FDU); FOTS applications 4005, 4408, 4669, 4962, 4822, and 5502]. The rats were anesthetized subcutaneously with a mixture (0.35-0.40 ml/100 g body weight) containing haloperidol (5 mg/ml; Janssen (Beerse, Belgium); 17% vol/vol), fentanyl (50 μg/ml; Actavis (Parsippany, NJ, USA); 25% vol/vol), and midazolam (5 mg/ml; Actavis; 25% vol/vol) in water. Rats received temgesic (0.33 ml/200 g body weight) and subcutaneous injection of NaCl (0.9%, 5-10 ml) after instillation of cells when needed, as judged by their condition.

Experimental Treatment Groups

The rats were treated 14 days after instillation of AY-27 cells or 33 days after ended 12-week exposure to BBN based on previous experience [16,20] and unpublished data. MMC (1 mg/ml) or bleomycin (1 mg/ml) was used for intravesical treatment, either alone or in combination with ATX-101 (30 μM). For the rats treated twice, treatments were performed on days 14 and 28. Controls were not treated (untreated) or sham treated with NaCl (0.9%). The bladder was washed with NaCl (0.9%, 1 × 0.3 ml) before instillation of the treatment solution (0.3 ml). The animals were turned every 15 minutes during the treatment. After 1 hour, the bladders were washed with NaCl (0.9%, 2 × 0.3 ml).

One hundred fifteen rats representing seven experimental/biologic replicas using the AY-27-model are included in the study and shown in Figure 4. Six rats are not included in the study due to death of unknown causes (five rats) or during anesthesia (one rat). Five rats had transparent and macroscopically normal bladders, i.e., they likely did not develop tumor after instillation of tumor cells ("no takes"). These rats were in groups treated with only NaCl (1 rat) and ATX-101 alone (all four rats below the broken line), as seen in Figure 4.

Thirty-one rats representing one experiment/biologic replica using the BBN model are included in the study and shown in Figure 4. All of these rats established tumor. One rat was not included in the study due to death of unknown cause.

We could not detect any side effects of the combination of MMC and ATX-101 compared to rats treated with MMC, ATX-101, or NaCl alone.

Termination

The rats from the AY-27 model were sacrificed 19 and 41 days after treatment, unless earlier in cases where the animals became ill

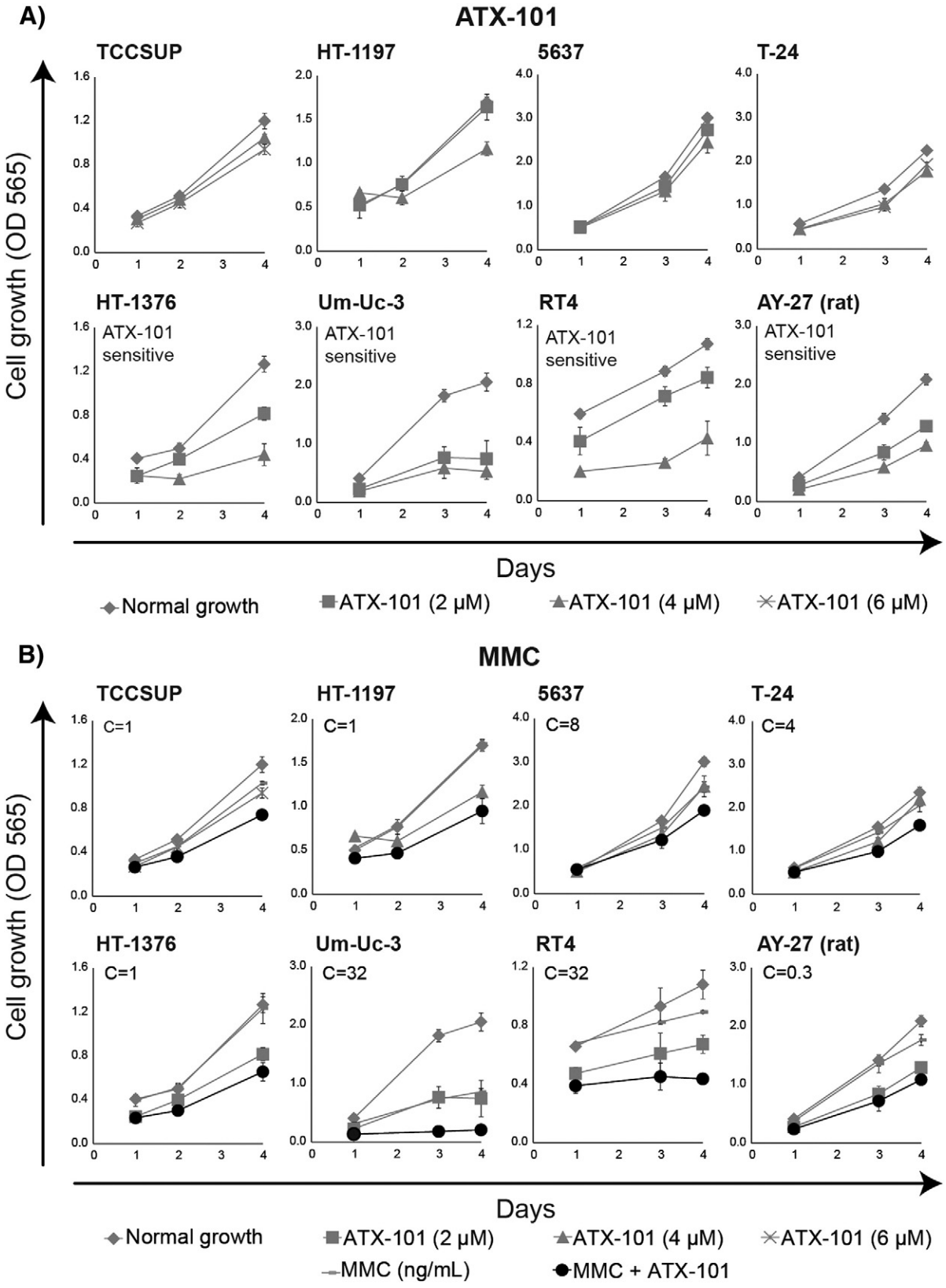

Figure 1. ATX-101 alone and in combination with MMC, bleomycin, and gemcitabine inhibits growth of human and rat bladder cancer cell lines. Cell growth over time of seven different human bladder cancer cell lines (TCCSUP, HT-1197, HT-1376, Um-Uc-3, 5637, T-25, and RT4) and one rat bladder cancer cell line (AY-27) was measured with 3-(4.5-dimethylthiazol-2-yl)-2.5 diphenyltetrazolium bromide assays. Growth of unexposed cells (—•—) as well as cells treated with ATX-101 [2 μM (—■—), 4 μM (—▲—), and 6 μM (—✳—)] and chemotherapeutic agents (MMC, bleomycin, or gemcitabine) alone (——) or in combination with ATX-101 (—●—) is marked. Data of one representative experiment of at least two are shown. Continuous exposure to (A) ATX-101, (B) ATX-101 and MMC alone or in combination, (C) ATX-101 and bleomycin alone or in combination, and (D) ATX-101 and gemcitabine alone or in combination.

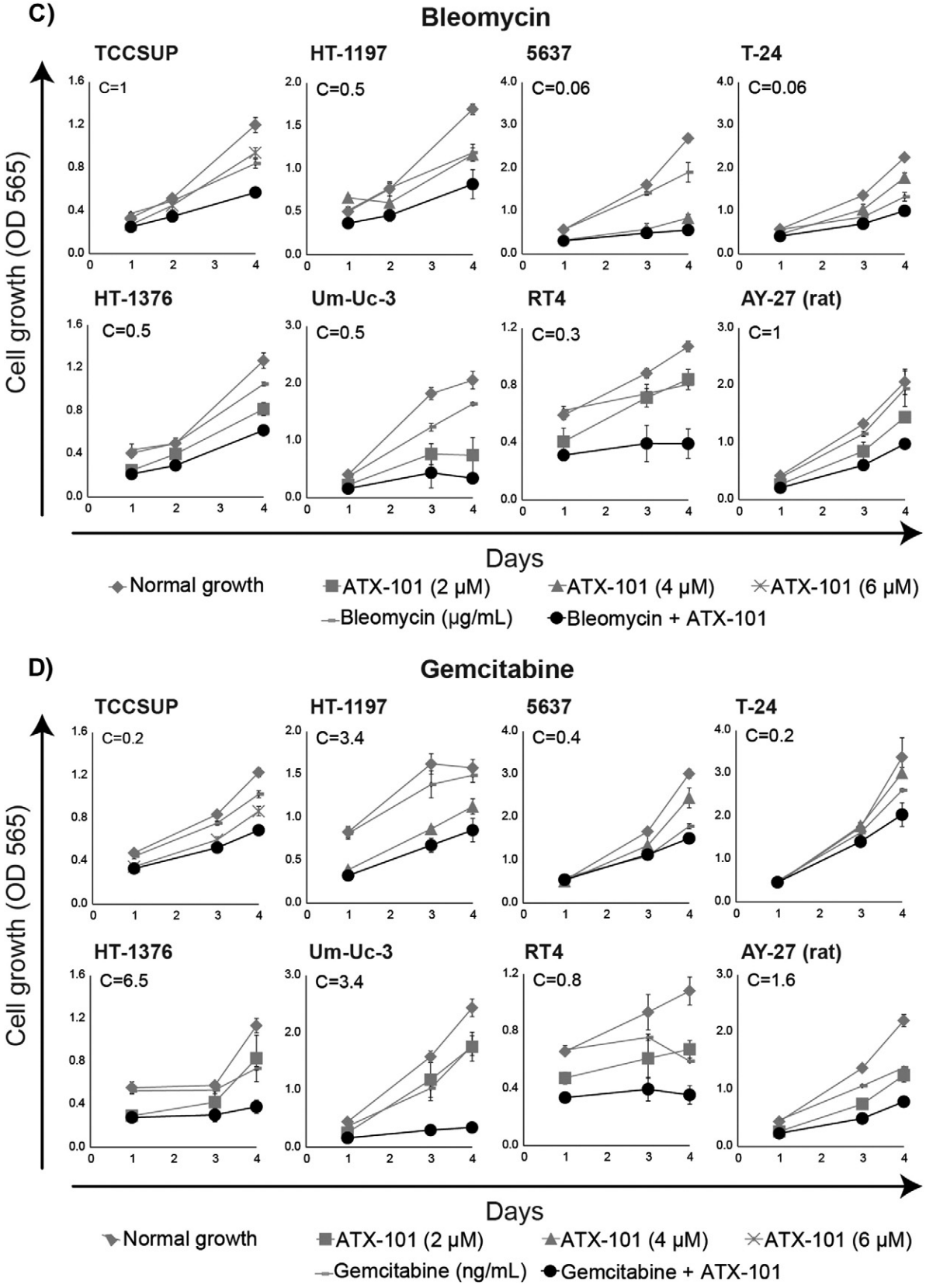

Figure 1. *(Continued)*

(marked by open symbols in Figure 4), while rats with endogenous tumors (BBN model) were sacrificed 115 days after treatment. The bladders were opened, weighed, and macroscopically examined before mounting and transferring to formalin (4%) for fixation, paraffin-embedding, and later histopathologic examination.

Statistics

Animals treated with bleomycin alone and bleomycin/ATX-101 showed a close to normal distribution; thus, a one tailed Student's *t* test was used for this experiment. For the animals treated with MMC alone and MMC/ATX-101, an overall larger effect of treatments was observed,

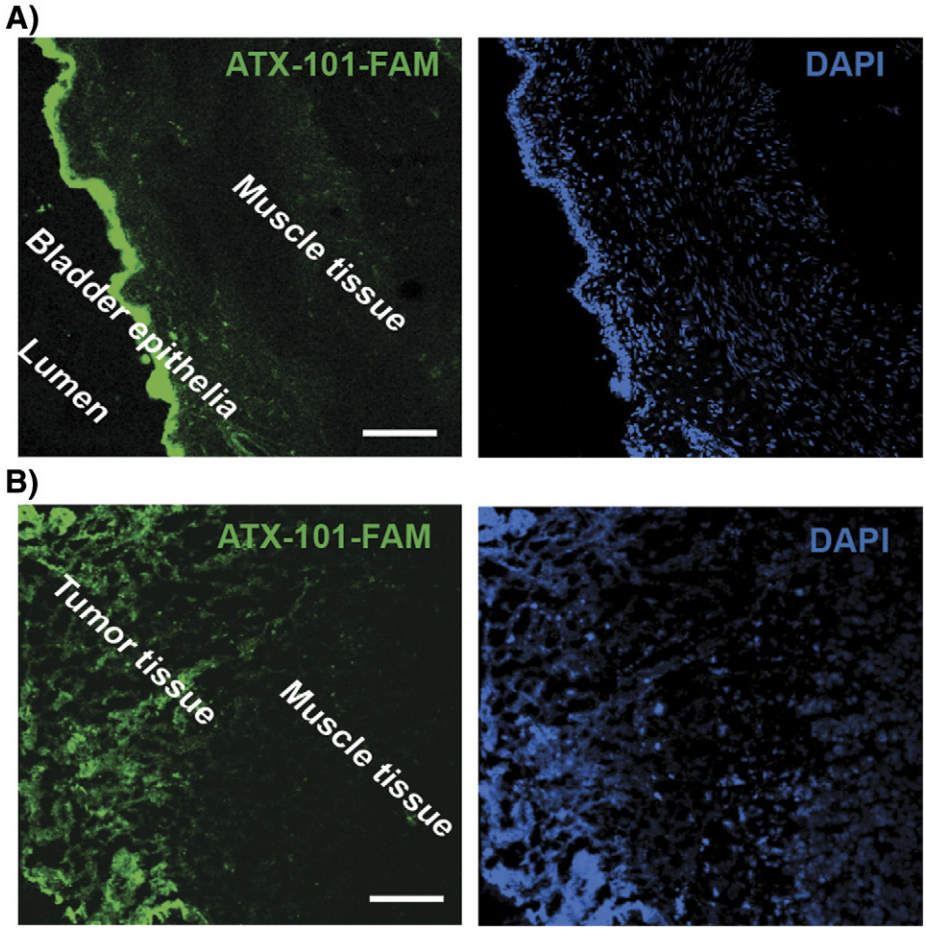

Figure 2. ATX-101 penetrates bladder epithelia and bladder cancer tissue. Penetration of FAM-tagged ATX-101 (30 μM; shown in green in the left panel) in bladder epithelia and cancer tissue after 1 hour intravesical instillation in rat bladders is shown. Frozen sections of ATX-101–FAM–treated bladders are DNA-stained with DAPI (shown in blue) and evaluated by confocal microscopy using a 20 × dry objective. (A) Normal bladder. (B) Tumor-bearing bladder. Bars, 100 μM.

and consequently, we observed a low bladder weight and a high bladder weight population. As verified macroscopically and by histopathologic examinations (Figure 3 and Table 1), the low weight population had stopped growing, whereas in the high weight population, the tumors were in active growth and this was the cause of the weight gain (not edema or inflammation). Therefore we used the χ^2 test on these two populations. In the AY-27 model, the "not growing" population was classified as the bladders below 0.23 g, based on the largest bladder in the low weight population at day 41 in the 2× treated MMC/ATX-101 group. In the BBN model, the "not growing" bladders had weights below 0.17 g. This is illustrated as broken lines in Figure 4.

Uptake Study

After intravesical instillation of ATX-101 (30 μM, 0.3 ml, 1 hour), the solutions were retrieved from the bladders, diluted (1:5) in HCl (0.2%), and analyzed for full-length peptide on a Waters Acquity I-Class UPLC – TQ-S triple quadrupole mass spectrometer operated in positive electrospray mode. The HPLC column was a Zorbax C_{18} 300SB Poroshell with dimensions of 2.1 × 75 mm. Column temperature was 40°C, and the flow rate was 0.4 ml/min. Mobile phases were 0.2% acetic acid + 0.01% trifluoroacetic acid in mass spectrometry (MS) grade water (A) and 0.2% acetic acid + 0.01% trifluoroacetic acid in MS grade acetonitrile (B). The following mobile phase gradient was used: 0 to 0.5 minutes, 0% B; 0.5 to 3 minutes, from 0% to 30% B; 3 to 3.5 minutes, from 30% to 100% B; 3.5 to 4 minutes, 100% B; 4 to 4.1 minutes, from 100% to 0% B, and 6 minutes. The Multiple Reaction Monitoring (MRM) transition 409.1→438.5 was used as a target ion for quantitation, and the MRM transitions 460.3→501.1 and 613.3→84.0 were used as qualifier ions with expected ratios of 0.3 and 0.6, respectively, to the target ion. Ion source settings were 1000 l/h, temperature of 500°C, and capillary cone voltage of 3 kV.

Penetration Study

After instillation of ATX-101 fluorescently tagged with either fluorescein (FAM) or cyanine-7 (Cy7) (30 μM, 0.3 ml, 1 hour), the bladders were washed with NaCl (0.9%, 3 × 0.3 ml). Frozen sections of ATX-101–FAM–treated bladders were DNA stained with 4′,6-diamidino-2-phenylindole (DAPI) and examined by confocal microscopy. Live animal imaging during instillation of ATX-101–Cy7 was performed using the Li-Cor small animal *in vivo* imaging system (170 μM resolution, Odyssey, CLx). After 1 hour, ATX-101–Cy7 was washed, and the imaging process was repeated.

Immunofluorescence and Confocal Imaging

Bladder cancer cells were grown on glass bottom dishes and stained with anti-PCNA (PC10; Santa Cruz Biotechnology Inc) and Alexa Fluor 532 goat anti-mouse (Invitrogen, Carlsbad, CA, USA) antibodies and DRAQ5 (eBioscience, San Diego, CA) as described [15]. The relative

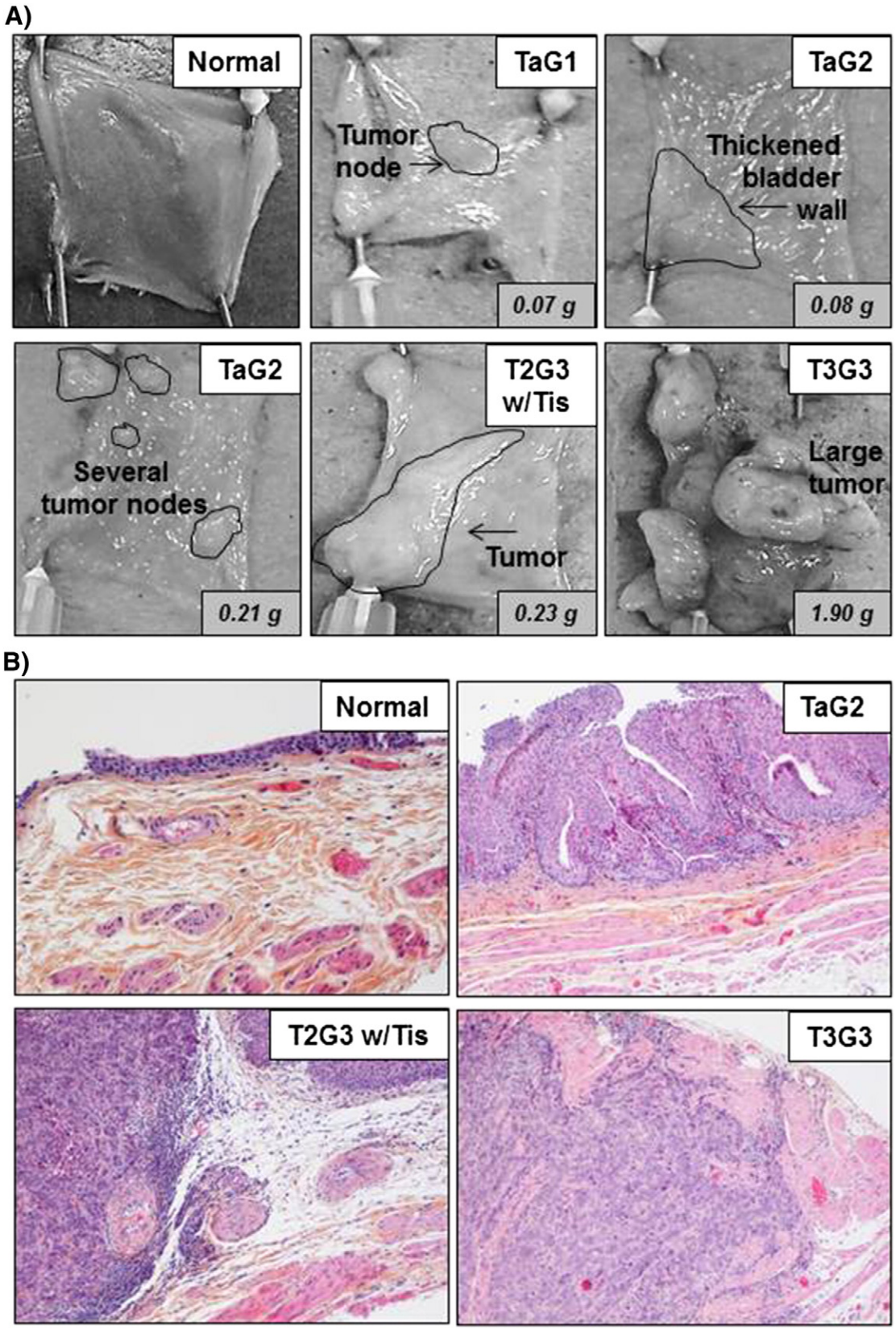

Figure 3. Macroscopic and HES-stained images of recovered normal and cancer-containing rat bladders (AY-27 model). (A) Images of opened and mounted rat bladders recovered from animals with different tumor grades as evaluated by histopathology. Bladder weights are given. (B) Images of HES-stained rat bladders (20 ×).

intensities of PCNA in cytosol/nuclei were calculated using mean region of interest containing at least 400 pixels using the Zeiss LSM 510 software.

Histopathologic Assessment

Slicing of freeze sections, paraffin embedding, and hematoxylin-erythrosine-saffron (HES) staining were done using standard procedures at the Cellular and Molecular Imaging Core Facility, NTNU. Frozen tissues were Optimal Cutting Temperature compound (OCT)-embedded, cut in 4-μm-thick sections, counterstained with DAPI (Vector, Burlingame, CA, USA), and examined in a Zeiss LSM 510 laser scanning microscope. The HES-stained tissues were examined for morphologic changes by a uropathologist using a light microscope. Immunohistochemistry: Formalin-fixed paraffin-embedded sections were deparaffinized before heat-induced epitope retrieval was performed using DAKO Target Retrieval Solution (S1699) and DAKO PT Link (Dako, Glostrup, Denmark). The sections were incubated for 40 minutes at room temperature with the proliferation marker anti-Ki67 (1:50; Abcam, Cambridge, UK; ab16667), the apoptosis marker anti–cleaved caspase-3 (Asp175; 1:100; Cell Signaling Technology, Beverly, MA, USA; #9661), and the senescence marker anti-p21 (10 μg/ml; Abcam; ab18209). Immunohistologic staining was performed using a DAKO Autostainer and DAKO EnVision Detection System with DAB+ chromogene. Sections were counterstained with hematoxylin. The immunohistochemistry-stained tissues were examined by a uropathologist.

Results

ATX-101 Increases the Sensitivity to Chemotherapeutic Drugs in Several Bladder Cancer Cell Lines

Prior studies have demonstrated that APIM peptides sensitize several different, but not all, cancer cell lines to chemotherapeutic agents [10,15]. To determine if bladder cancer is a good indication, we tested a panel of human bladder cancer cell lines for growth after exposure to ATX-101 alone in combination with three functionally different chemotherapeutics that each induces different DNA lesions. We found that three of the seven cancer cell lines tested (HT-1376, Um-Uc-3, and RT4) in addition to the rat bladder cancer cell line AY-27 were highly sensitive to ATX-101 alone (Figure 1*A*). In addition, all the cell lines showed an increased sensitivity toward all the three cytotoxic compounds tested (gemcitabine, a nucleoside analog; bleomycin, a DNA strand break inducer; MMC, introducing ICLs) when combined with ATX-101 (Figure 1, *B* to *D*, *black circles*). These data suggest that treatments of bladder cancer could benefit from treatment with ATX-101 in combination with several different chemotherapeutics.

ATX-101 Penetrates into the Bladder Wall

The ability of a drug to penetrate the bladder wall mucosa as well as underlying tissue is imperative for its efficacy in bladder cancer therapy. ATX-101 is rapidly imported into cells in cell cultures [15]. To examine ATX-101's penetration into the bladder wall, we measured residual full-length ATX-101 in retrieved solution after intravesical bladder instillation by liquid chromatography - mass spectrometry/mass spectrometry (LC-MS/MS). We found an approximately 10-fold reduction in full-length peptide: 53 μg/ml ATX-101 in instilled solution *versus* 5.7 ± 1.6 μg/ml in retrieved solutions (n = 8). The closed catheter was kept in place during instillation, and no leakage was observed. Urine dilution of the samples could account for up to two- to three-fold reduction in peptide concentrations, and ATX-101 has a $T_{1/2}$ of 5.5 hours in undiluted urine (human) *in vitro* (data not shown). Therefore, the data suggested that ATX-101 penetrates the bladder wall, and to confirm this, we instilled fluorescently tagged ATX-101 (ATX-101–FAM). Confocal images confirmed that ATX-101 was distributed throughout the bladder epithelia and penetrated into the muscular layer. Furthermore, ATX-101 efficiently penetrated into tumor-containing areas (Figure 2, *A* and *B*).

The ability of ATX-101 to penetrate the bladder wall was also examined by live animal imaging. Fluorescently tagged ATX-101 (ATX-101–Cy7) could clearly be detected in the bladder area, whereas no diffusion outside this region of the animal was observed during the instillation (data not shown). ATX-101–Cy7 could also be detected in the same region of the animal after washing of the bladder with saline, supporting the presence of residual peptide in the bladder wall.

ATX-101 Potentiates the Efficacy of Bleomycin and MMC in Two Orthotopic Rat Bladder Cancer Models

Next, we examined the anticancer effect of ATX-101 in combination with bleomycin and MMC in the AY-27 syngeneic rat orthotopic bladder cancer model. The rats were treated once intravesically with chemotherapeutics alone or in combination with ATX-101. The tumor load in the bladders 19 and 41 days after treatment was evaluated by total bladder weight in combination with macroscopic (Figure 3*A*) and histopathologic examination (Table 1 and Figure 3*B*). We observed reduced tumor load in animals treated with ATX-101 in combination with bleomycin (Figure 4*A*) or MMC (Figure 4*B*) compared to treatment with bleomycin or MMC alone. Reduced tumor load in the groups receiving the combination of MMC/ATX-101 was observed both after 19 and 41 days. Additionally, we treated two groups twice (2×) with the combination MMC/ATX-101 or MMC alone and examined the groups 41 days after the first treatment. Again, increased efficacy was observed in the

Figure 4. Inhibition of tumor growth in two orthotopic bladder cancer models in immune-competent rats after treatment of ATX-101 in combination with bleomycin and MMC. Rats were treated once or twice (2 ×) through intravesical instillation (1 hour) of MMC (1 mg/ml, 3 mM) or bleomycin (1 mg/ml, 75 μM) alone or in combination with ATX-101 (30 μM). The number of animals (n) in each experimental treatment group is given below the x-axis. Animals that died/were sacrificed before termination date are marked with open symbols. (A) The AY-27-model: bleomycin alone and in combination with ATX-101. (B) The AY-27-model: MMC alone and in combination with ATX-101. The control groups (untreated, 0.9% NaCl, and normal bladders) are the same in A and B. Animals were sacrificed, and bladders were harvested and evaluated for tumor presence by total weight at day 19 or 41 post-treatment. (C) The BBN model: intravesical treatment with MMC alone or in combination with ATX-101. Animals were sacrificed, and bladders were harvested and evaluated for tumor presence by total weight 115 days post-treatment. Error bars represent SEM. Statistics: (A) P values were calculated by the unpaired, two-tailed Student's t test. (B and C) Broken lines divide the actively growing and not growing tumors, and the χ^2 test was used to calculate P values between the different groups (described in the Materials and Methods section).

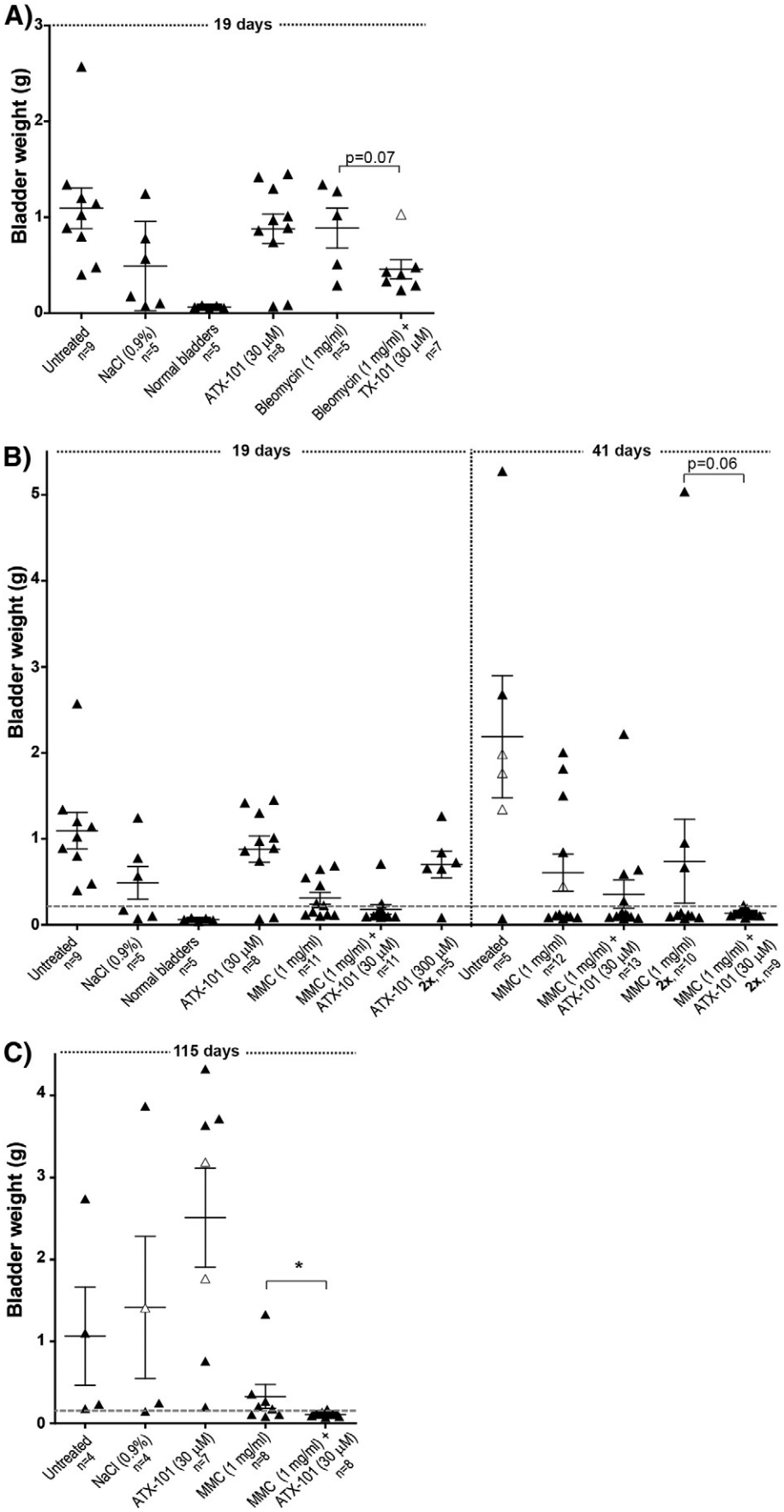
A)
19 days
Bladder weight (g)
p=0.07
Untreated n=9
NaCl (0.9%) n=5
Normal bladders n=5
ATX-101 (30 µM) n=8
Bleomycin (1 mg/ml) n=5
Bleomycin (1 mg/ml) + TX-101 (30 µM) n=7
B)
19 days
41 days
p=0.06
Bladder weight (g)
Untreated n=9
NaCl (0.9%) n=5
Normal bladders n=5
ATX-101 (30 µM) n=8
MMC (1 mg/ml) n=11
MMC (1 mg/ml) + ATX-101 (30 µM) n=11
ATX-101 (300 µM) 2x, n=5
Untreated n=5
MMC (1 mg/ml) n=12
MMC (1 mg/ml) + ATX-101 (30 µM) n=13
MMC (1 mg/ml) 2x, n=10
MMC (1 mg/ml) + ATX-101 (30 µM) 2x, n=9
C)
115 days
Bladder weight (g)
*
Untreated n=4
NaCl (0.9%) n=4
ATX-101 (30 µM) n=7
MMC (1 mg/ml) n=8
MMC (1 mg/ml) + ATX-101 (30 µM) n=8

Table 1. Histopathologic Evaluation of Rat Bladders Retrieved from AY-27 and BBN Models

A

AY27 Groups	Histology results	Bladder weight (g)
Control	No tumor	0.06
No treatment, 19d	T3G3	1.9
ATX-101, 19d	T3G3	0.86
ATX-101, 19d	T2G3	1.45
MMC, 19d	TaG1	0.117
MMC, 19d	T2G3 and Tis	0.225
MMC, 19d	T1G3	0.15
MMC, 19d	T3G3	0.548
ATX-101+MMC, 19d	TaG1	0.144
ATX-101+MMC, 19d	Tis	0.096
ATX-101+MMC, 19d	TaG1 and Tis	0.105
ATX-101+MMC, 19d	Tis	0.095
ATX-101+MMC, 19d	Tis	0.107
ATX-101+MMC, 19d	T2G3 and Tis	0.246
ATX-101+MMC, 19d	T1G3	0.13
ATX-101+MMC, 19d	T1G3 and Tis	0.142
ATX-101+MMC, 19d	TaG2 and Tis	0.088
ATX-101+MMC, 19d	TaG1 and Tis	0.096
ATX-101+MMC, 41d	TaG1 and Tis	0.093
ATX-101+MMC, 41d	Tis	0.088
ATX-101+MMC, 41d	Tis	0.111
ATX-101+MMC, 41d	TaG2	0.276
ATX-101+MMC, 41d	T1G3 and Tis	0.127
ATX-101+MMC, 41d	T2G3	0.14
ATX-101+MMC, 41d	No tumor	0.1
ATX-101+MMC, 41d	Tis	0.11
ATX-101+MMC, 41d	Ta	0.59

B

BBN Groups		Histology results	Bladder weight (g)
No treatment	a	T1G3	1.102
	b	T1G2	
No treatment		T1G2	0.232
ATX-101		T1G2	0.197
ATX-101	a	T1G2	3.632
	b	T1G3	
	c	TaG3	
ATX-101		TaG2	0.758
MMC		TaG1	0.107
MMC		T2G3 and Tis	0.176
MMC		TaG1	0.226
MMC		TaG2	0.081
MMC		TaG2	0.105
MMC		TaG2	0.206
MMC		T3G3	1.328
MMC		TaG1	0.356
ATX-101+MMC		TaG1	0.073
ATX-101+MMC		TaG2 and Tis	0.092
ATX-101+MMC		No tumor	0.116
ATX-101+MMC		TaG1	0.08
ATX-101+MMC		TaG1	0.102
ATX-101+MMC		TaG2	0.172
ATX-101+MMC		TaG1 and Tis	0.137
ATX-101+MMC		TaG1	0.112

C

AY27 Groups	Histology results	Bladder weight (g)	Staining in tumor area: ki67	p21	caspase 3
ATX-101+MMC, 2x, 41d	T2G3 and Tis	0.227	~10%	<5%	+
ATX-101+MMC, 2x, 41d	No tumor	0.148	<5% *	-	-
ATX-101+MMC, 2x, 41d	Tis	0.105	~5%	~10%	+
MMC, 2x, 41d	T3G3	0.952	+	~10%	+
MMC, 2x, 41d	Tis	0.112	~5%	>50%	+
MMC, 2x, 41d	T3G3	0.668	+	<5%	+

+=> 70 % positive
*= in the basal layer

MMC/ATX-101 combination group *versus* MMC alone ($P = .06$) supporting the results from the animals treated once (Figure 4*C*). We could not detect any single agent activity of ATX-101 neither after one or two treatments nor after increasing the dose 10-fold (Figure 4*C*) even though ATX-101 had single agent activity on AY-27 in cell culture (Figure 1).

The AY-27 model is based on instillation of a cancer cell line and it can, therefore, be considered a "monoclonal" rapidly growing tumor model. We also wanted to examine if ATX-101 increased the efficacy of MMC in a more "endogenous" slow growing tumor model. In this model, tumors are induced by adding BBN to the drinking water. Intravesical treatment was done with MMC alone or in combination with ATX-101 in exactly the same manner as in the previous AY-27 model. These rats were then kept for an additional 115 days before termination of the study. Similar to the results from the AY-27 model, ATX-101 in combination with MMC reduced the tumor growth compared to MMC alone ($P = .007$; Figure 4*D*). Thus, these two models together strongly suggest that ATX-101 potentially improves the anticancer efficacy of MMC.

Histopathologic Examination Suggests that ATX-101 Potentiates the Effect of Intravesical Chemotherapeutics

The macroscopic (Figure 3*A*) and histopathologic examination (Figure 3*B* and Table 1) verified that the bladder weight measurements corresponded overall well with the tumor status of the bladders. All animals not treated with MMC or MMC/ATX-101 developed T2-3G3 in the AY-27 group and Ta/1G2-3 in the BBN group (Table 1, *A* and *B*).

One rat in each of the MMC/ATX-101 combination groups (both BBN and AY-27) contained no detectable tumors, only metaplasia as determined histopathologically (Table 1). The macroscopic evaluation of these bladders at time of harvest suggested that the bladder wall was less transparent than normal bladders supporting that there had been a tumor previously.

The combination treatment of MMC/ATX-101 in the BBN model resulted in mostly TaG1-classified tumors, whereas MMC treatment alone resulted in more high-grade tumor classifications, ranging from TaG1 to T3G3 tumors (Table 1*B*). The histologic evaluation of the bladders from the AY-27 studies had a similar tendency, i.e., less invasive/smaller bladder tumors in the group treated with the combination of MMC/ATX-101 (Table 1, *A* and *C*).

The data of bladder weights (Figure 4, *B* and *C*) suggests that small tumors below the broken line have stopped growing as there is no increase in bladder weights observed between days 19 and 41. To test this, we selected three animals from the groups treated twice with MMC or MMC/ATX-101 and examined them for caspase-3, Ki67, and p21 levels. One rat treated twice with MMC/ATX-101 was tumor free and was negative for caspase-3 and p21. Tumors in the other bladders containing small tumors were positive for caspase-3 and expressed low levels of p21 and Ki67, supporting lack of growth

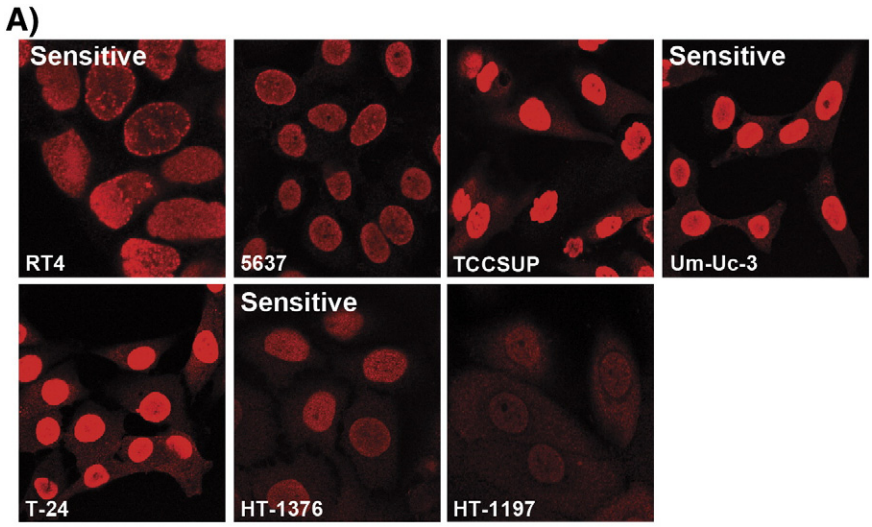

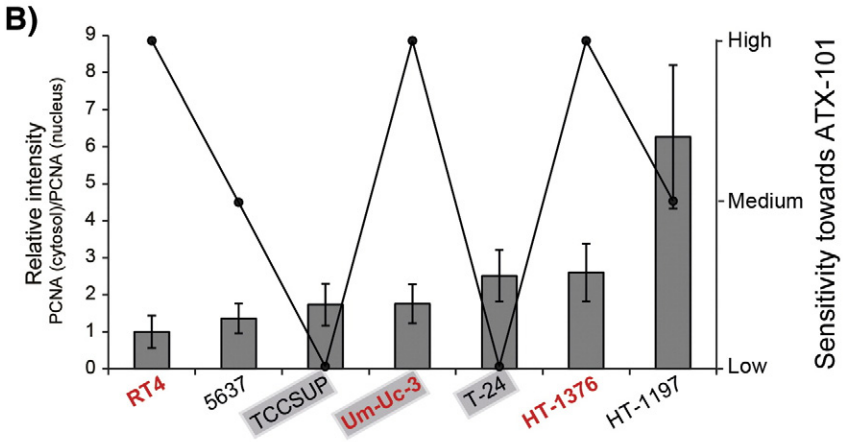

C)

Cell lines :	RT4	5637	TCCSUP	Um-Uc-3	T-24	HT-1376	HT-1197
IC30-50:							
MMC (ng/mL)	32	8	1	32	4	1	1
Bleomycin (mg/mL)	0.3	0.06	1	0.5	0.08	0.5	0.5
Gemcitabine (ng/mL)	0.8	0.4	0.2	0.4	0.2	6.25	3.4

Figure 5. PCNA levels in human bladder cancer cell lines do not correlate with ATX-101 sensitivity. (A) Confocal fluorescence images of immunofluorescently stained PCNA (red) in the human bladder cancer panel. The images are taken the same day using the same settings on the microscope; thus, fluorescence intensity directly corresponds to different levels of PCNA. (B) Left *y*-axis: relative levels of PCNA in the cytosol over PCNA in the nucleus in the different cell lines. Mean intensities of cytosolic and nuclear PCNA in four regions of interest in each cell, from 13 cells, from each cell line are measured. Values are normalized against the value in RT4 (the cell line with lowest ratio of cytosolic /nuclear PCNA; gray bars, mean ± SEM, $n = 52$). Right *y*-axis: sensitivity toward ATX-101 as a single agent. The bladder cancer cell lines were classified as high, medium, or low according to their sensitivity toward ATX-101 based on results from the cell survival assays (Figure 1). A graph indicating sensitivity is shown. (C) Doses of MMC, bleomycin, and gemcitabine giving 30% to 50% (40 ± 10) reduction in growth in the different cell lines (from data in Figure 1 and biologic replicas) are summarized and compared to sensitivity toward ATX-101 and PCNA content in the cells. (B and C) Cell lines in red are sensitive to ATX-101 and cell lines with high total levels of PCNA are shown with gray background.

(Table 1*C*), whereas the large tumor in the MMC 2× group was positive for Ki67, supporting active growth.

The Sensitivity of Bladder Cancer Cells to ATX-101 Is Not Linked to PCNA Levels

PCNA is often used as a marker for proliferation and is often overexpressed in cancer cells [21]. Additionally, PCNA has vital roles in processes frequently deregulated in cancer, e.g., DNA replication and repair/chromatin remodeling and apoptosis [5,6,15]. It is also reported that the expression of PCNA is upregulated in BBN-induced bladder tumors in rats similar to what is found in superficial bladder cancers in humans [22]. Thus, intracellular levels of PCNA [23] and/or localization of PCNA (i.e., levels in cytosol *vs* nuclei) could potentially be a biomarker for whether the bladder cancer cells are sensitive to ATX-101 or not. Therefore, we examined the PCNA content and distribution in the bladder cancer panel and compared it

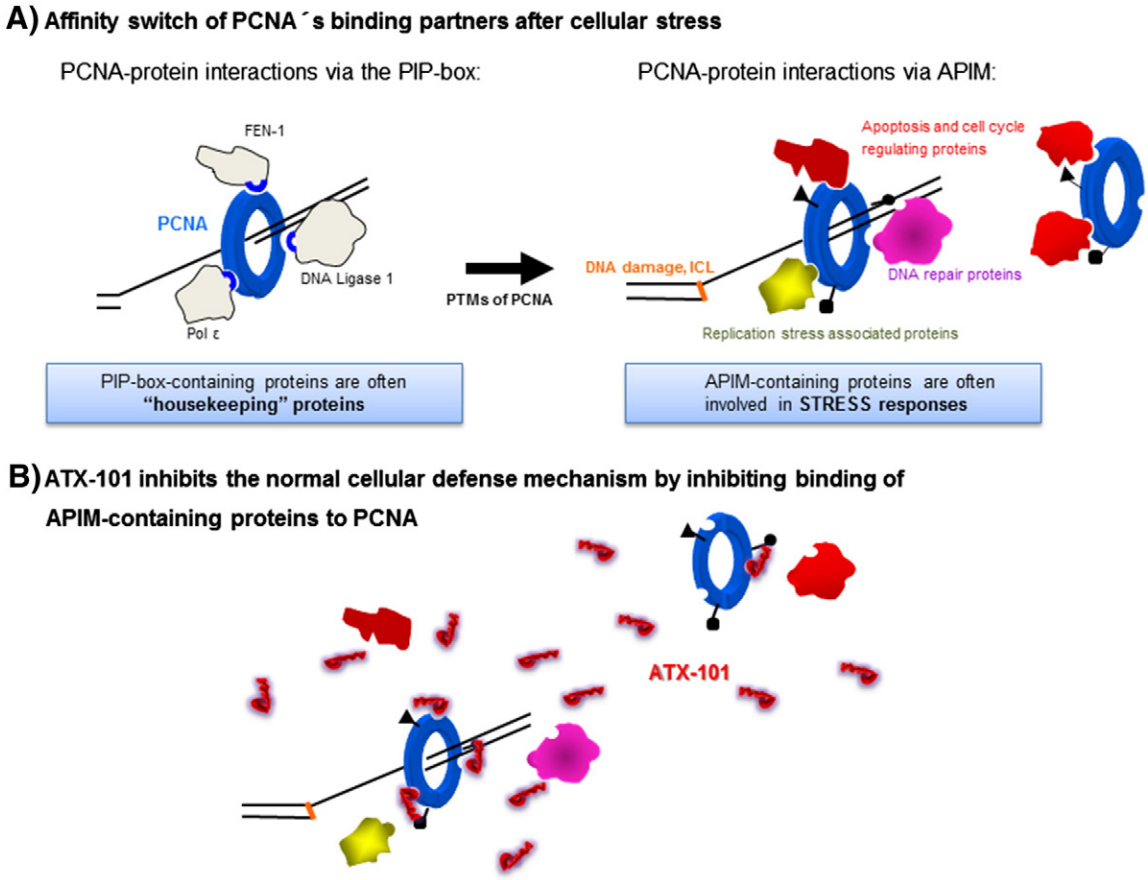

Figure 6. Model. PCNA (blue ring) is an essential cellular protein controlling cellular homeostasis. "Housekeeping" proteins such as proteins necessary for replication (gray proteins) interact with PCNA through a sequence known as the PIP box (A, left). Upon cellular stress such as DNA damage, PCNA is posttranslationally modified ("PTMs", addition of black groups on PCNA) and this targets a stress switch increasing the affinities for APIM-containing proteins (yellow, pink, and red proteins; A, right). Upon targeting PCNA with peptides containing the APIM motif such as ATX-101 (in red), APIM-containing proteins are prohibited from PCNA interaction (B). This impairs cellular homeostasis and renders cancer cells hypersensitive to a multiple of chemotherapeutic drugs.

to sensitivity against ATX-101 and the other chemotherapeutics. We found that the sensitivity toward ATX-101 (line in Figure 5*B*, *right axis*; cell lines marked in red are ATX-101 sensitive) is not correlated to the ratio of cytosolic *versus* nuclear PCNA (bars in Figure 5*B*, *left axis*) or to total levels of PCNA in the cells (cell lines with gray background). Furthermore, there is no correlation between high PCNA content (gray background), ATX-101 sensitivity (red), and the cell's sensitivity to MMC, bleomycin, and gemcitabine (summarized in Figure 5*C*).

Discussion

We found no correlation between bladder cancer cells sensitivity toward ATX-101, or the other chemotherapeutics tested, and PCNA levels. Experiments have shown that APIM peptides co-immunoprecipitated a subfraction of PCNA with a different isoelectric profile compared to the isoelectric profile of total PCNA in cells [10]. During replicative stress/arrest, PCNA is posttranslationally modified enabling a switch from the replicative to the TLS polymerases [5,24]. We believe that the stress levels in the cancer cells and thus the posttranslational modifications on PCNA determine the sensitivity of cells toward ATX-101 and not the total level of PCNA or ratios of PCNA in cytosol/nucleus. Nonmalignant cells are not to the same degree "stressed" and therefore only require housekeeping proteins for continued survival, whereas malignant cells are in a stressed state and therefore critically dependent on stress response proteins [25]. This explains the selectivity of ATX-101's ability to selectively target cancer cells and the low overall cytotoxicity *in vivo* [15].

A model suggesting a switch from normal housekeeping proteins binding PCNA through the PIP box to stress response proteins binding through APIM during stress is illustrated in Figure 6. The molecular mechanism of how ATX-101 sensitizes cancer cells toward chemotherapeutics is multimodal and based on ATX-101's ability to target PCNA and inhibit interactions between APIM-containing proteins and PCNA [15]. It has been shown that APIM-PCNA interaction is important for the efficacy to repair specific DNA lesions [10,11] and to restart stalled replication forks [12,13]. Recently, the APIM-PCNA interaction was shown to be important for the functionality of TFII-I in TLS [14]. Additionally, attenuated interaction of PCNA with other APIM-containing proteins such as the homologous recombination protein RAD51B, Topo II alpha, and the translesion polymerase POLζ will likely also reduce the "stressed" cancer cells' ability to repair DNA lesions.

Many new cancer drugs are selected for their cytotoxic effects on the rapidly proliferating cancer cell lines used in preclinical experiments. When it comes to clinical phase II, these drugs often fail because primary cancers do not proliferate as rapidly as cancer cell

lines [26]. Our group has previously demonstrated that the induction of apoptosis and increased efficacy of ICL-inducing drugs caused by ATX-101 is not S-phase dependent; however, normal cells are far less sensitive than cancer cells [15]. Thus, ATX-101 likely increases the efficacy of MMC in all cancer cells independent of their cycle phase, and this is likely the reason for the good anticancer efficacy of the MMC/ATX-101 combination observed also in the slow growing cancers induced by BBN.

ATX-101 has previously been shown to reduce DNA repair and increase apoptotic/cytotoxic responses to chemotherapeutics *in vitro* and *in vivo* [10,11,15]. This study shows that ATX-101 penetrated the bladder wall and increased the anticancer efficacy of intravesically dosed bleomycin and MMC. The results are confirmed in two fundamentally different orthotopic bladder cancer models in immune-competent rats. The BBN model, which induced genetically heterogeneous and slow growing cancers, is potentially more relevant to the human bladder cancer disease than the AY-27 cancer cell line–based model. Therefore, we regard the results observed in this model as very promising and supportive for future clinic trials of ATX-101/MMC in patients with NMIBC.

Acknowledgments

We thank Kathrin Torseth from the Cellular and Molecular Imaging Core Facility, NTNU and the personnel from the Comparative Medicine Core Facility, NTNU for technical assistance.

References

[1] Babjuk M, Oosterlinck W, Sylvester R, Kaasinen E, Böhle A, Palou-Redorta J, and Rouprêt M (2011). EAU guidelines on non–muscle-invasive urothelial carcinoma of the bladder, the 2011 update. *Eur Urol* **59**, 997–1008.

[2] Shelley MD, Mason MD, and Kynaston H (2010). Intravesical therapy for superficial bladder cancer: a systematic review of randomised trials and meta-analyses. *Cancer Treat Rev* **36**, 195–205.

[3] Tomasz M (1995). Mitomycin C: small, fast and deadly (but very selective). *Chem Biol* **2**, 575–579.

[4] Clauson C, Scharer OD, and Niedernhofer L (2013). Advances in understanding the complex mechanisms of DNA interstrand cross-link repair. *Cold Spring Harb Perspect Biol* **5**(10), a012732.

[5] Mailand N, Gibbs-Seymour I, and Bekker-Jensen S (2013). Regulation of PCNA–protein interactions for genome stability. *Nat Rev Mol Cell Biol* **14**, 269–282.

[6] Witko-Sarsat V, Mocek J, Bouayad D, Tamassia N, Ribeil JA, Candalh C, Davezac N, Reuter N, Mouthon L, and Hermine O, et al (2010). Proliferating cell nuclear antigen acts as a cytoplasmic platform controlling human neutrophil survival. *J Exp Med* **207**, 2631–2645.

[7] Rosental B, Brusilovsky M, Hadad U, Oz D, Appel MY, Afergan F, Yossef R, Rosenberg LA, Aharoni A, and Cerwenka A, et al (2011). Proliferating Cell Nuclear Antigen Is a Novel Inhibitory Ligand for the Natural Cytotoxicity Receptor NKp44. *J Immunol* **187**, 5693–5702.

[8] Naryzhny SN and Lee H (2010). Proliferating cell nuclear antigen in the cytoplasm interacts with components of glycolysis and cancer. *FEBS Lett* **584**, 4292–4298.

[9] Warbrick E (1998). PCNA binding through a conserved motif. *Bioessays* **20**, 195–199.

[10] Gilljam KM, Feyzi E, Aas PA, Sousa MM, Müller R, Vågbø CB, Catterall TC, Liabakk NB, Slupphaug G, and Drablos F, et al (2009). Identification of a novel, widespread, and functionally important PCNA-binding motif. *J Cell Biol* **186**, 645–654.

[11] Gilljam KM, Müller R, Liabakk NB, and Otterlei M (2012). Nucleotide Excision Repair Is Associated with the Replisome and Its Efficiency Depends on a Direct Interaction between XPA and PCNA. *PLoS One* **7**, e49199.

[12] Ciccia A, Nimonkar AV, Hu Y, Hajdu I, Achar YJ, Izhar L, Petit SA, Adamson B, Yoon JC, and Kowalczykowski C (2012). Polyubiquitinated PCNA recruits the ZRANB3 translocase to maintain genomic integrity after replication stress. *Mol Cell* **47**, 396–409.

[13] Bacquin A, Pouvelle C, Siaud N, Perderiset M, Salome-Desnoulez S, Tellier-Lebegue C, Lopez B, Charbonnier JB, and Kannouche PL (2013). The helicase FBH1 is tightly regulated by PCNA via CRL4(Cdt2)-mediated proteolysis in human cells. *Nucleic Acids Res* **41**, 6501–6513.

[14] Fattah FJ, Hara K, Fattah KR, Yang C, Wu N, Warrington R, Chen DJ, Zhou P, Boothman DA, and Yu H (2014). The Transcription Factor TFII-I Promotes DNA Translesion Synthesis and Genomic Stability. *PLoS Genet* **10**, e1004419.

[15] Muller R, Misund K, Holien T, Bachke S, Gilljam KM, Vatsveen TK, Ro TB, Bellacchio E, Sundan A, and Otterlei M (2013). Targeting proliferating cell nuclear antigen and its protein interactions induces apoptosis in multiple myeloma cells. *PLoS One* **8**, e70430.

[16] Arum CJ, Anderssen E, Viset T, Kodama Y, Lundgren S, Chen D, and Zhao CM (2010). Cancer immunoediting from immunosurveillance to tumor escape in microvillus-formed niche: a study of syngeneic orthotopic rat bladder cancer model in comparison with human bladder cancer. *Neoplasia* **12**, 434–442.

[17] Xiao Z, McCallum T, Brown K, Miller G, Halls S, Parney I, and Moore R (1999). Characterization of a novel transplantable orthotopic rat bladder transitional cell tumour model. *Br J Cancer* **81**, 638–646.

[18] Larsen EL, Randeberg LL, Gederaas OA, Arum CJ, Hjelde A, Zhao CM, Chen D, Krokan HE, and Svaasand LO (2008). Monitoring of hexyl 5-aminolevulinate-induced photodynamic therapy in rat bladder cancer by optical spectroscopy. *J Biomed Opt* **13**(4), 044031.

[19] Kunze E and Schauer A (1977). Morphology, classification and histogenesis of N-butyl-N-(4-hydroxybutyl)-nitrosamine-induced carcinomas in the urinary bladder of rats. *Z Krebsforsch Klin Onkol* **88**, 273–289.

[20] Bryan GT (1977). The pathogenesis of experimental bladder cancer. *Cancer Res* **37**, 2813–2816.

[21] Helleday T, Petermann E, Lundin C, Hodgson B, and Sharma RA (2008). DNA repair pathways as targets for cancer therapy. *Nat Rev Cancer* **8**, 193–204.

[22] Ariel I, Ayesh S, Gofrit O, Ayesh B, Abdul-Ghani R, Pizov G, Smith Y, Sidi AA, Birman T, and Schneider T (2004). Gene expression in the bladder carcinoma rat model. *Mol Carcinog* **41**, 69–76.

[23] Stoimenov I and Helleday T (2009). PCNA on the crossroad of cancer. *Biochem Soc Trans* **37**, 605–613.

[24] Lehmann AR, Niimi A, Ogi T, Brown S, Sabbioneda S, Wing JF, Kannouche PL, and Green CM (2007). Translesion synthesis: Y-family polymerases and the polymerase switch. *DNA Repair (Amst)* **6**, 891–899.

[25] Hills SA and Diffley JF (2014). DNA Replication and Oncogene-Induced Replicative Stress. *Curr Biol* **24**, R435-444.

[26] Chan KS, Koh CG, and Li HY (2012). Mitosis-targeted anti-cancer therapies: where they stand. *Cell Death Dis* **3**, e411.